Appendix: Position-based Elastic Rod

submission #1006

1 Property of a Darboux vector

Let us assume frame $\mathbf{D} = \left[\mathbf{d}^1, \mathbf{d}^2, \mathbf{d}^3\right]$ is parametrized by $s \in \mathbb{R}$. Darboux vector is defined as

$$\boldsymbol{\omega} = \frac{1}{2}\sum_{i=1}^{3} \mathbf{d}^i \times \mathbf{d}^{i\prime}, \tag{1}$$

where $\mathbf{d}^{i\prime} = \partial \mathbf{d}^i / \partial s$. Using the Darboux vector, the each axis of the frame can be written as

$$\mathbf{d}^{k\prime} = \boldsymbol{\omega} \times \mathbf{d}^k, \quad k = 1, 2, 3. \tag{2}$$

here is the proof for $k = 1$

$$\begin{aligned}
\boldsymbol{\omega} \times \mathbf{d}^1 &= \frac{1}{2}\left(\mathbf{d}^1 \times \mathbf{d}^{1\prime} + \mathbf{d}^2 \times \mathbf{d}^{2\prime} + \mathbf{d}^3 \times \mathbf{d}^{3\prime}\right) \times \mathbf{d}^1, && (3)\\
&= +\frac{1}{2}\left\{(\mathbf{d}^{1T}\mathbf{d}^1)\mathbf{d}^{1\prime} - (\mathbf{d}^{1\prime T}\mathbf{d}^1)\mathbf{d}^1\right\} \\
&\quad +\frac{1}{2}\left\{(\mathbf{d}^{2T}\mathbf{d}^1)\mathbf{d}^{2\prime} - (\mathbf{d}^{2\prime T}\mathbf{d}^1)\mathbf{d}^2\right\} \\
&\quad +\frac{1}{2}\left\{(\mathbf{d}^{3T}\mathbf{d}^1)\mathbf{d}^{3\prime} - (\mathbf{d}^{3\prime T}\mathbf{d}^1)\mathbf{d}^3\right\}, && (4)\\
&= \frac{1}{2}\left\{\mathbf{d}^{1\prime} + (\mathbf{d}^{1\prime T}\mathbf{d}^2)\mathbf{d}^2 + (\mathbf{d}^{1\prime T}\mathbf{d}^2)\mathbf{d}^3\right\}, && (5)\\
&= \frac{1}{2}\left\{\mathbf{d}^{1\prime} + \sum_{i=1}^{3}(\mathbf{d}^{1\prime T}\mathbf{d}^i)\mathbf{d}^i\right\}, && (6)\\
&= \mathbf{d}^{1\prime}. && (7)
\end{aligned}$$

The coordinate of the Darboux vector to the axis $\mathbf{d}_1$ can be written as:

$$\begin{aligned} \omega_1 &= \boldsymbol{\omega} \cdot \mathbf{d}^1 && (8) \\ &= \frac{1}{2}\left(\mathbf{d}^1 \times \mathbf{d}^{1\prime} + \mathbf{d}^2 \times \mathbf{d}^{2\prime} + \mathbf{d}^3 \times \mathbf{d}^{3\prime}\right) \cdot \mathbf{d}^1, && (9) \\ &= \frac{1}{2}\left\{(\mathbf{d}^1 \times \mathbf{d}^2) \cdot \mathbf{d}^{2\prime} + (\mathbf{d}^1 \times \mathbf{d}^3) \cdot \mathbf{d}^{3\prime}\right\}, && (10) \\ &= \frac{1}{2}\left\{\mathbf{d}^3 \cdot \mathbf{d}^{2\prime} - \mathbf{d}^2 \cdot \mathbf{d}^{3\prime}\right\}, && (11) \\ &= \mathbf{d}^3 \cdot \mathbf{d}^{2\prime} = -\mathbf{d}^2 \cdot \mathbf{d}^{3\prime}. && (12) \end{aligned}$$

Similarly, we can write coordinate value of the Darboux vector for axis $\mathbf{d}_2$ and $\mathbf{d}_3$ as:

$$\begin{aligned} \omega_2 &= \boldsymbol{\omega} \cdot \mathbf{d}^2, && (13) \\ &= \mathbf{d}^1 \cdot \mathbf{d}^{3\prime} = -\mathbf{d}^3 \cdot \mathbf{d}^{1\prime}. && (14) \end{aligned}$$

$$\begin{aligned} \omega_3 &= \boldsymbol{\omega} \cdot \mathbf{d}^3, && (15) \\ &= \mathbf{d}^2 \cdot \mathbf{d}^{1\prime} = -\mathbf{d}^1 \cdot \mathbf{d}^{2\prime}. && (16) \end{aligned}$$

As a result, these relationships hold

$$\begin{aligned} \mathbf{d}^{1\prime} &= \omega_3 \mathbf{d}^2 - \omega_2 \mathbf{d}^3, && (17) \\ \mathbf{d}^{2\prime} &= \omega_1 \mathbf{d}^3 - \omega_3 \mathbf{d}^3, && (18) \\ \mathbf{d}^{3\prime} &= \omega_2 \mathbf{d}^1 - \omega_1 \mathbf{d}^2. && (19) \end{aligned}$$

2 Rotation matrix and Axis-Angle vector

Rotation matrix $\mathbf{R} \in SO(3)$ between two frames $\mathbf{D}_a$ and $\mathbf{D}_b$ can be written as

$$\mathbf{R} = {\mathbf{D}_a}^T \mathbf{D}_b. \qquad (20)$$

The element of this rotation matrix can be written as:

$$R_{ij} = \sum_{k=1}^{3} [\mathbf{D}_a]_{ki} [\mathbf{D}_b]_{kj} = \mathbf{d}_a^i \cdot \mathbf{d}_b^j, \qquad (21)$$

where $\mathbf{D}_a = [\mathbf{d}_a^1, \mathbf{d}_a^2, \mathbf{d}_a^3] \in \mathbb{R}^{3\times 3}$.

Let's think about axis angle representation $\theta\mathbf{n}$ (where $|\mathbf{n}| = 1$) of the rotation matrix $\mathbf{R}$. From Rogorigues's formula, we can write rotation matrix using axis vector $\mathbf{n}$ and angle θ as:

$$\mathbf{R} = \mathbf{I} + \tilde{\mathbf{n}} \sin\theta + (1 - \cos\theta)(\mathbf{n}\mathbf{n}^T - \mathbf{I}) \tag{22}$$

Below are the relationships between rotation matrices and their bases and axis angle representation.

$$\mathrm{tr}\mathbf{R} = \sum_{n=1}^{3} \mathbf{d}_a^n \cdot \mathbf{d}_b^n = 3 + (1 - \cos\theta)(1 - 3) = 1 - 2\cos\theta \tag{23}$$

$$\cos\theta = \frac{1}{2}\left\{ (\sum_{n=1}^{3} \mathbf{d}_a^n \cdot \mathbf{d}_b^n) - 1 \right\} = \frac{\mathrm{tr}\mathbf{R} - 1}{2} \tag{24}$$

$$\tilde{\mathbf{n}} \sin\theta = \frac{1}{2}(R - R^T) \tag{25}$$

$$\begin{aligned}
\mathbf{n}\sin\theta &= \frac{1}{2} vect\left(R - R^T\right) && (26)\\
&= \frac{1}{2}\left(R_{32} - R_{23}, R_{13} - R_{31}, R_{21} - R_{12}\right)^T && (27)\\
&= \frac{1}{2}\sum_{k=1}^{3}\left\{ \begin{array}{c} D_a^{k3} D_b^{k2} - D_a^{k2} D_b^{k3} \\ D_a^{k1} D_b^{k3} - D_a^{k3} D_b^{k1} \\ D_a^{k2} D_b^{k1} - D_a^{k2} D_b^{k2} \end{array} \right\} && (28)\\
&= \frac{1}{2}\sum_{k=1}^{3} \mathbf{d}_a^k \times \mathbf{d}_b^k && (29)
\end{aligned}$$

$$\begin{aligned}
2\mathbf{n}\tan\frac{\theta}{2} &= \frac{2\mathbf{n}\sin\theta}{\cos\theta + 1} && (30)\\
&= \frac{2vect\left(\mathbf{R} - \mathbf{R}^T\right)}{1 + \mathrm{tr}\mathbf{R}} && (31)\\
&= \frac{2\sum_{k=1}^{3} \mathbf{d}_a^k \times \mathbf{d}_b^k}{1 + \sum_{n=1}^{3} \mathbf{d}_a^n \cdot \mathbf{d}_b^n} && (32)
\end{aligned}$$

3 Differentiation of constraints

3.1 Constraints for each edge

For simplicity, we consider an edge with two end points $\mathbf{p}_0$ and $\mathbf{p}_1$ which has a ghost point $\mathbf{p}_2$. We denote mid point of the edge as $\mathbf{p}_m = (\mathbf{p}_0 + \mathbf{p}_1)/2$.

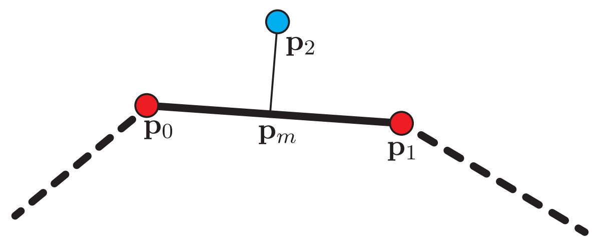

Figure 1: Configurations of points on a edge

3.1.1 Edge length constraint

As the equation (18) in the paper, the constraint to maintain edge length as the rest length can be written as:

$$C^L(\mathbf{p}_0, \mathbf{p}_1) = |\mathbf{p}_0 - \mathbf{p}_1| - \bar{L}. \tag{33}$$

Hence, the derivative with respect to the two end points of the edge becomes:

$$\nabla_{\mathbf{p}_0} C^L = \frac{\mathbf{p}_0 - \mathbf{p}_1}{|\mathbf{p}_0 - \mathbf{p}_1|}, \quad \nabla_{\mathbf{p}_1} C^L = \frac{\mathbf{p}_1 - \mathbf{p}_0}{|\mathbf{p}_1 - \mathbf{p}_0|} \tag{34}$$

These result in the point updates:

$$\begin{cases} \Delta\mathbf{p}_0 & = & -\frac{w_0}{w_0+w_1}(|\mathbf{p}_0 - \mathbf{p}_1| - \bar{L})\frac{\mathbf{p}_0-\mathbf{p}_1}{|\mathbf{p}_0-\mathbf{p}_1|}, \\ \Delta\mathbf{p}_1 & = & -\frac{w_1}{w_0+w_1}(|\mathbf{p}_0 - \mathbf{p}_1| - \bar{L})\frac{\mathbf{p}_1-\mathbf{p}_0}{|\mathbf{p}_1-\mathbf{p}_0|}. \end{cases} \tag{35}$$

3.1.2 Perpendicular bisector constraint on the ghost point

As the equation (19) in the paper, the constraint to maintain the ghost point to be located in the perpendicular bisector of the edge can be written as:

$$\begin{cases} \nabla_{\mathbf{p}_0} C^P & = & \mathbf{p}_0 - \mathbf{p}_2, \\ \nabla_{\mathbf{p}_1} C^P & = & \mathbf{p}_2 - \mathbf{p}_1, \\ \nabla_{\mathbf{p}_2} C^P & = & \mathbf{p}_1 - \mathbf{p}_0. \end{cases} \tag{36}$$

The Lagrange multiplier becomes

$$\lambda = \frac{(\mathbf{p}_2 - \mathbf{p}_m)^T(\mathbf{p}_1 - \mathbf{p}_0)}{w_0|\mathbf{p}_0 - \mathbf{p}_2|^2 + w_1|\mathbf{p}_2 - \mathbf{p}_1|^2 + w_2|\mathbf{p}_1 - \mathbf{p}_0|^2}. \tag{37}$$

The resulting point updates becomes

$$\begin{cases} \Delta\mathbf{p}_0 & = & -\lambda w_0(\mathbf{p}_0 - \mathbf{p}_2), \\ \Delta\mathbf{p}_1 & = & -\lambda w_1(\mathbf{p}_2 - \mathbf{p}_1), \\ \Delta\mathbf{p}_2 & = & -\lambda w_2(\mathbf{p}_1 - \mathbf{p}_0). \end{cases} \tag{38}$$

3.1.3 Distance constraint between a ghost point and an edge

We enforce a constraint which keeps the ghost point at a same distance $\bar{L}^g$ form an edge. As the equation (20) in the paper, the constraint is given as:

$$C^D = (\mathbf{p}_0, \mathbf{p}_1, \mathbf{p}_2) = |\mathbf{p}_m - \mathbf{p}_2| - \bar{L}^g. \tag{39}$$

The differentiation of this constraint can be computed as

$$\begin{cases} \nabla_{\mathbf{p}_0} C^D & = & -0.5(\mathbf{p}_2 - \mathbf{p}_m)/|\mathbf{p}_2 - \mathbf{p}_m|, \\ \nabla_{\mathbf{p}_1} C^D & = & -0.5(\mathbf{p}_2 - \mathbf{p}_m)/|\mathbf{p}_2 - \mathbf{p}_m|, \\ \nabla_{\mathbf{p}_2} C^D & = & +1.0(\mathbf{p}_2 - \mathbf{p}_m)/|\mathbf{p}_2 - \mathbf{p}_m|, \end{cases} \tag{40}$$

where $\mathbf{p}_{m2} = \mathbf{p}_2 - \mathbf{p}_0$. The Lagrange multiplier becomes:

$$\lambda = \frac{|(\mathbf{p}_2 - \mathbf{p}_m)| - \bar{l}_g}{0.25w_0 + 0.25w_1 + w_2} \tag{41}$$

Finally, the points are updated as:

$$\begin{cases} \Delta\mathbf{p}_0 & = & +0.5w_0\lambda(\mathbf{p}_2 - \mathbf{p}_m)/|\mathbf{p}_2 - \mathbf{p}_m| \\ \Delta\mathbf{p}_1 & = & +0.5w_1\lambda(\mathbf{p}_2 - \mathbf{p}_m)/|\mathbf{p}_2 - \mathbf{p}_m| \\ \Delta\mathbf{p}_2 & = & -1.0w_2\lambda(\mathbf{p}_2 - \mathbf{p}_m)/|\mathbf{p}_2 - \mathbf{p}_m| \end{cases} \tag{42}$$

3.1.4 Derivative of the coordinate bases

A material frame basis vectors are defined on a edge as the equation (3) in the paper. We compute differentiation of these basis vector with respect to the points.

$$\begin{cases} \partial\mathbf{d}^3/\partial\mathbf{p}_0 & = & -\frac{1}{|\mathbf{p}_{01}|}(\mathbf{I} - \mathbf{d}^3 \otimes \mathbf{d}^3), \\ \partial\mathbf{d}^3/\partial\mathbf{p}_1 & = & +\frac{1}{|\mathbf{p}_{01}|}(\mathbf{I} - \mathbf{d}^3 \otimes \mathbf{d}^3), \\ \partial\mathbf{d}^3/\partial\mathbf{p}_2 & = & 0 \end{cases} \tag{43}$$

$$
\begin{cases}
\partial \mathbf{d}^2/\partial \mathbf{p}_0 &= \frac{1}{|\mathbf{p}_{01}\times\mathbf{p}_{02}|}(\mathbf{I}-\mathbf{d}^2\otimes\mathbf{d}^2)[\mathbf{p}_2-\mathbf{p}_1], \\
\partial \mathbf{d}^2/\partial \mathbf{p}_1 &= \frac{1}{|\mathbf{p}_{01}\times\mathbf{p}_{02}|}(\mathbf{I}-\mathbf{d}^2\otimes\mathbf{d}^2)[\mathbf{p}_0-\mathbf{p}_2], \\
\partial \mathbf{d}^2/\partial \mathbf{p}_2 &= \frac{1}{|\mathbf{p}_{01}\times\mathbf{p}_{02}|}(\mathbf{I}-\mathbf{d}^2\otimes\mathbf{d}^2)[\mathbf{p}_1-\mathbf{p}_0].
\end{cases} \tag{44}
$$

$$
\begin{cases}
\partial \mathbf{d}^1/\partial \mathbf{p}_0 &= -[\mathbf{d}^3]\partial\mathbf{d}^2/\partial\mathbf{p}_0 + [\mathbf{d}^2]\partial\mathbf{d}^3/\partial\mathbf{p}_0, \\
\partial \mathbf{d}^1/\partial \mathbf{p}_1 &= -[\mathbf{d}^3]\partial\mathbf{d}^2/\partial\mathbf{p}_1 + [\mathbf{d}^2]\partial\mathbf{d}^3/\partial\mathbf{p}_1, \\
\partial \mathbf{d}^1/\partial \mathbf{p}_2 &= -[\mathbf{d}^3]\partial\mathbf{d}^2/\partial\mathbf{p}_2
\end{cases} \tag{45}
$$

3.2 Derivative of Modified Darboux Vector

Let we have a orientation element that connects edge A and edge B as shown in Figure 2. There are five points $(\mathbf{p}_a, \mathbf{p}_b, \mathbf{p}_c, \mathbf{p}_d, \mathbf{p}_e)$ involved in this orientation element. Here A_i means the internal labeling of the points inside edge A and similarly B_i labels the points inside edge B.

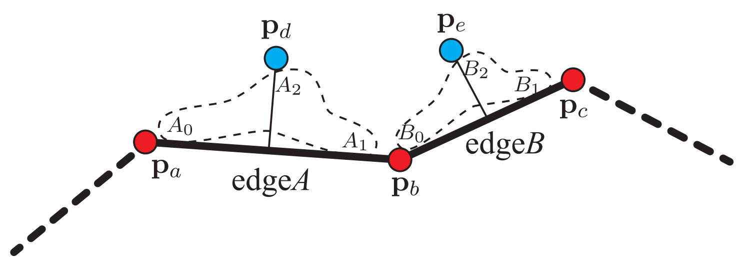

Figure 2: Configurations of points on a edge

As the equation (10) in the paper, our modified Darboux vector can be written as

$$
\Omega_i = \left(\frac{2}{\bar{l}}\right)\frac{{\mathbf{d}_A^j}^T\mathbf{d}_B^k - {\mathbf{d}_A^k}^T\mathbf{d}_B^j}{1+\sum_{n=1}^{3}{\mathbf{d}_A^n}^T\mathbf{d}_B^n}, \tag{46}
$$

Because our constraint enforcement procedure isn't affected by scaling this modified Darboux vector, we can let $\bar{l} = 1$ for simplicity. With the chain rule, we obtain following derivative of Darboux vector:

$$\begin{aligned}
\Omega_i' &= X\left({\mathbf{d}_B^k}^T {\mathbf{d}_A^j}' - {\mathbf{d}_B^j}^T {\mathbf{d}_A^k}'\right) \\
&- X\left({\mathbf{d}_A^k}^T {\mathbf{d}_B^j}' - {\mathbf{d}_A^j}^T {\mathbf{d}_B^k}'\right) \\
&- \frac{1}{2} X\Omega_i \left(\sum_{n=1}^{3} {\mathbf{d}_B^n}^T {\mathbf{d}_A^n}' + {\mathbf{d}_A^n}^T {\mathbf{d}_B^n}'\right), \qquad (47)
\end{aligned}$$

where $X = 2/(1 + \sum_{n=1}^{3} {\mathbf{d}_A^n}^T \mathbf{d}_B^n)$.

Let us denote the derivative of coordinate basis vector with respect to the position of a point in each edge as:

$$\mathbf{D}_{A_i}^j = \frac{\partial \mathbf{d}_A^j}{\partial \mathbf{p}_{A_i}}, \qquad \mathbf{D}_{B_i}^j = \frac{\partial \mathbf{d}_B^j}{\partial \mathbf{p}_{B_i}} \qquad (48)$$

We have explained how to compute these derivative in Section 3.1.4. Using these notations, the derivatives of the Darboux vector with respect to the five points become:

$$\begin{aligned}
\partial\Omega_i/\partial\mathbf{p}_a &= +X\left({\mathbf{d}_B^k}^T \mathbf{D}_{A_0}^j - {\mathbf{d}_B^j}^T \mathbf{D}_{A_0}^k\right) - \frac{1}{2} X\Omega_i \left(\sum_{n=1}^{3} {\mathbf{d}_B^n}^T \mathbf{D}_{A_0}^n\right) \quad (49) \\
\partial\Omega_i/\partial\mathbf{p}_b &= +X\left({\mathbf{d}_B^k}^T \mathbf{D}_{A_1}^j - {\mathbf{d}_B^j}^T \mathbf{D}_{A_1}^k\right) - \frac{1}{2} X\Omega_i \left(\sum_{n=1}^{3} {\mathbf{d}_B^n}^T \mathbf{D}_{A_1}^n\right) \\
&\quad -X\left({\mathbf{d}_A^k}^T \mathbf{D}_{B_0}^j - {\mathbf{d}_A^j}^T \mathbf{D}_{B_0}^k\right) - \frac{1}{2} X\Omega_i \left(\sum_{n=1}^{3} {\mathbf{d}_A^n}^T \mathbf{D}_{B_0}^n\right) \quad (50) \\
\partial\Omega_i/\partial\mathbf{p}_c &= -X\left({\mathbf{d}_A^k}^T \mathbf{D}_{B_1}^j - {\mathbf{d}_A^j}^T \mathbf{D}_{B_1}^k\right) - \frac{1}{2} X\Omega_i \left(\sum_{n=1}^{3} {\mathbf{d}_A^n}^T \mathbf{D}_{B_1}^n\right) \quad (51) \\
\partial\Omega_i/\partial\mathbf{p}_d &= +X\left({\mathbf{d}_B^k}^T \mathbf{D}_{A_2}^j - {\mathbf{d}_B^j}^T \mathbf{D}_{A_2}^k\right) - \frac{1}{2} X\Omega_i \left(\sum_{n=1}^{3} {\mathbf{d}_B^n}^T \mathbf{D}_{A_2}^n\right) \quad (52) \\
\partial\Omega_i/\partial\mathbf{p}_e &= -X\left({\mathbf{d}_A^k}^T \mathbf{D}_{B_2}^j - {\mathbf{d}_A^j}^T \mathbf{D}_{B_2}^k\right) - \frac{1}{2} X\Omega_i \left(\sum_{n=1}^{3} {\mathbf{d}_A^n}^T \mathbf{D}_{B_2}^n\right) \quad (53)
\end{aligned}$$

4 Algorithm Overview

The overall algorithm is outlined in Algorithm 1. Here, "#iterations" means the number of constraint-enforcement iterations. Note that we handle contact and damping using the same techniques as in [MHHR07].

Algorithm 1: Simulation Step

$t \Leftarrow t + \Delta t$ // step time

forall the *points i* **do**

  $\mathbf{v}_i \Leftarrow \mathbf{v}_i + \Delta t\mathbf{g}$ // apply gravity

forall the *edge e* **do** // modify gravity on ghost points

  $\mathbf{v}_m^t \Leftarrow 0.5(\mathbf{v}_{e-1} + \mathbf{v}_e)$

  $\mathbf{a}_m \Leftarrow (\mathbf{v}_m^t - \mathbf{v}_m^{t-\Delta t})/\Delta t$

  $r \Leftarrow (\mathbf{a}_m \cdot \mathbf{g})/|\mathbf{g}|^2$

  $\mathbf{v}_e^g \Leftarrow \mathbf{v}_e^g - (1-r)\Delta t\mathbf{g}$

  $\mathbf{v}_{e-1} \Leftarrow \mathbf{v}_{e-1} + 0.5(1-r)\Delta t\mathbf{g}$

  $\mathbf{v}_e \Leftarrow \mathbf{v}_e + 0.5(1-r)\Delta t\mathbf{g}$

forall the *points i* **do**

  $\mathbf{x}_i^* \Leftarrow \mathbf{x}_i + \Delta t\mathbf{v}_i$ // predict position

while *iter* $<$ *#iterations* **do**

  forall the *edge e* **do**

    update $\mathbf{x}^*$ for the C_e^L, C_e^P, C_e^D // (18)(19)(20) in the paper

  forall the *orientation element e* **do**

    update $\mathbf{x}^*$ for the $\mathbf{C}_e^{BT}$ // (21) in the paper

  forall the *tip of rods* **do**

    update $\mathbf{x}^*$ for the $\mathbf{C}^O$,C^T // (23)(24) in the paper

forall the *points i* **do**

  $\mathbf{v}_i \Leftarrow (\mathbf{x}_i^* - \mathbf{x}_i)/\Delta t$ // update velocity

  $\mathbf{x}_i^* \Leftarrow \mathbf{x}_i$ // update position

5 Preservation of rotational momentum

We compare the behavior of a straight rod when three different methods are used to apply gravity to ghost points. The first method is to apply the standard gravity force to each ghost point. The second method is to applying no gravity force to the ghost points. The third method is our gravity force modification technique (see Section 6 in the paper). We simulated two simple scenes with a straight rod; hanging down and free-fall.

As shown in Fig. 3, the first method shows an artifact of curved static deformation. This is because the side of the rod with ghost points is heavier than the other sides. The second method gains rotational momentum during free-fall because the ghost points are "pulling up" the rod from one side. Our gravity force modification approach does not exhibit such artifacts.

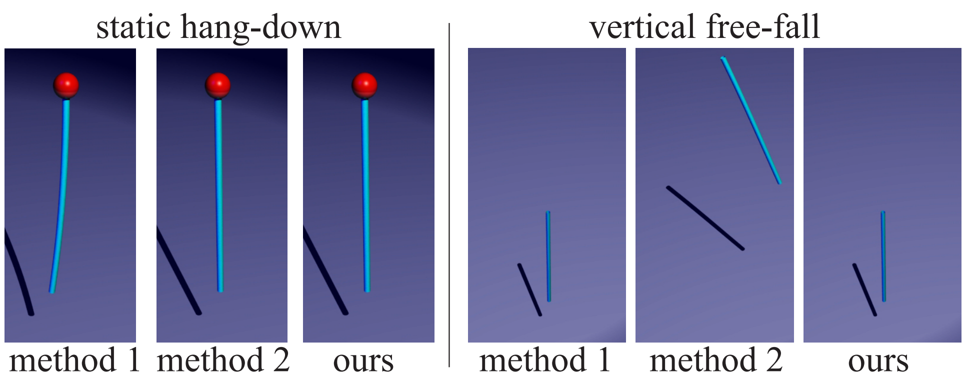

Figure 3: Simulations of a straight rod (**left**) hangs down and (**right**) falls down with three methods to apply gravity on ghost points: full gravity force (method 1), no gravity force (method 2), and our modified gravity force.

References

[MHHR07] Müller M., Heidelberger B., Hennix M., Ratcliff J.: Position based dynamics. *Visual Communication and Image Representation 18*, 2 (2007).